ISSN: 2455-2631 June 2023 IJSDR | Volume 8 Issue 6

Design and Optimization of FSAE Wheel Assembly Using Finite Elemental Analysis

[1]Yasin Sayyed, [2]Nayan Patil, [3]Kiran Mhetre, [4]Bhargav Patil, [5]Yash Salunke, [6]Saurabh Kale, [7]Shyam Sonawane

[1,2,3,4,5,6] UG Students, [7]Associate Professor
Department of Mechanical Engineering,
Government College of Engineering and
Research Awasari(kh), Pune, India

Abstract- **The wheel assembly is a main role in the performance of the Overall vehicle when dynamic situations are to be Considered. In this research work, parametric modeling and finite elemental analysis have been used to design and optimize the wheel assembly. The component has been designed using an analytical method. Manufacturing methods have been discussed for precision manufacturing of assembly. A complete CAD model of the wheel assembly is followed by a Top-down assembly modeling approach. The simulation results will be used to evaluate the strength, stiffness, and durability of the components, and to identify potential areas for improvement.**

Index Terms- **King-pin inclination, Scrub radius, Knuckle, Centrifugal Force, Wheel hub, Rotor Disc, petals.**

I. INTRODUCTION

Fundamentally FSAE is a sport in which mid-scale open-body four-wheeled vehicles races with each other. There are many kinds of variants of Formula vehicles available out of which are internal combustion engine powered and some are electrified with motors. Although the vehicle dynamics and control systems moreover remain common to both the vehicles. Focusing on the wheel assembly, the wishbones which is the main link between the chassis and the knuckle of the vehicle. The basic dynamic terms of knuckle assembly of a Go-Kart should be understood as follows,

Camber – There are three kinds of camber, positive camber, negative camber, and neutral camber. The illustration of the camber can see in Figure 1. Positive camber is when the center axis of the wheel leans outward the vehicle about the perpendicular axis to the ground and vice-versa of negative camber. In the neutral camber wheel axis and perpendicular to the ground, the axis coincides with each other and a complete ground patch can be observed.

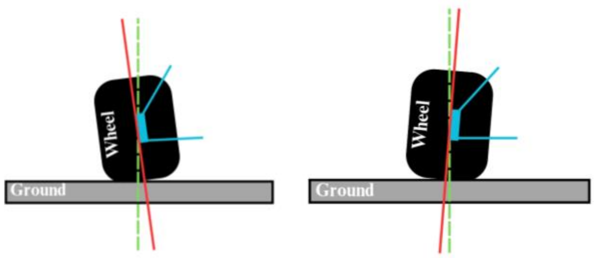

(a) Positive camber (b) Negative camber
Fig. 1 Types of camber

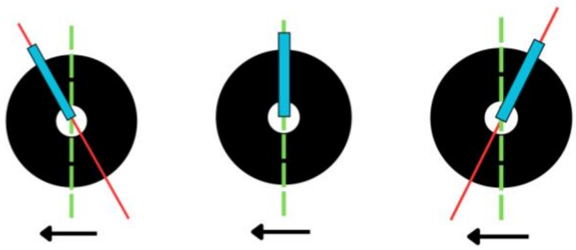

(a) Negative caster (b) Neutral caster (c) Positive caster
Fig. 2 Types of casters

Caster – Caster can be observed from the side view of the kart. There are three kinds of casters as follows; Neutral caster, positive caster, and negative caster. The illustration of the caster can see in Figure 2. The negative caster–center axis of the knuckle tilted forward about a vertical ground axis, the neutral caster–center axis of the knuckle coincides with the vertical ground axis, and the positive caster–center axis of the knuckle titled backward about a vertical ground axis.

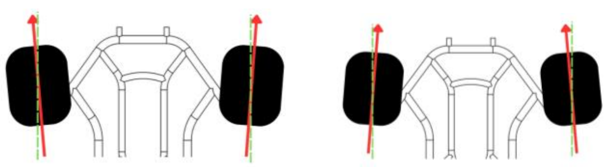

(a) Toe-out (b) Toe-in

Fig. 3 Toe in and out condition
(a) Toe-out (b) Toe-in

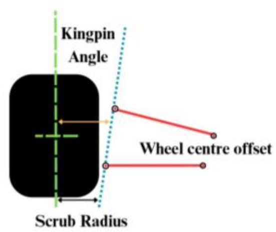

Fig. 4 Kingpin inclination

Toe - When the front tires are pointing straight ahead, an angle called the toe is generated. Toe in and toe out is the two conceivable toe situations. Toe-in is the term used when the center lines of the wheel tend to meet in front of the direction of motion of the vehicle. Toe-out is the term used when the lines tend to meet behind the vehicle's direction of motion. The illustrations can be seen in Figure 3. Kingpin inclination - Two lines—one in the center of the tire and the other in the center of the upright were used to calculate the kingpin angle. The scrub radius is the distance, when viewed from the front, between the center of the wheel's contact patch and the kingpin axis, where both should touch the ground.

II. COMPREHENSIVE WHEEL ASSEMBLY DESIGN

For the vehicle to move, the knuckle joins the control arms to the hub and the hub to the wheels. The knuckle is also connected to the steering arm and caliper, which enable the driver to steer and stop the car, respectively. Direct connections between the hub and the wheel and the knuckle are made. The hub must rotate with the wheel while the knuckle must remain motionless with respect to the chassis. The exploded view of the designed assembly is shown in Figure 5.

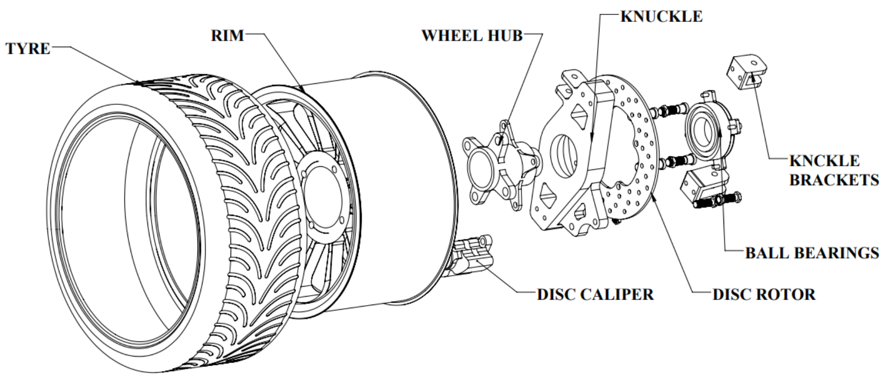

Fig. 5 Complete wheel assembly

Some standard physical parameters have been selected for design considerations as shown in table 1.

Table 1. Physical parameters taken into design consideration

Physical parameters	**Values**
King Pin Inclination	8 degrees
Caster Angle	4 degrees
Tie Rod Angle	6 degrees
Track Width	1100mm rear, 1060 mm front
Wheel Diameter	520.4 mm
Total length of Knuckle	240 mm (Rim of diameter 330 mm)
Upper A-arm angle	(- 3) degrees
Lower A-arm angle	0

A. Upright Design

The topologically optimized model of the upright is shown in Figure 6. The upright is the component of the wheel assembly that is pressed onto the spindle, and it is also where the double wishbones are mounted. The knuckle's additional purpose is to serve as a mounting point for the brake calliper. Since it was decided that the hub and spindle would be one component the effective spindle dimensions were driven by the selected bearing. To keep the bearing in its proper axial position, utilize a bearing lock.

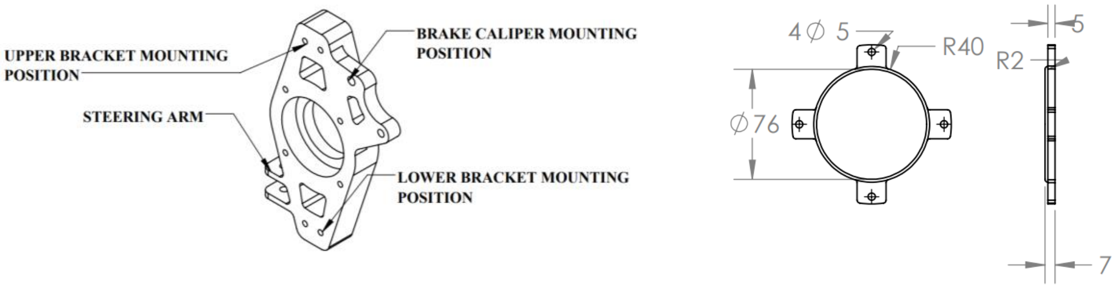

Fig. 6 Upright and bearing lock

Longitudinal Forces during Braking -
While braking, the weight of the rear side tends to come in the front side of the vehicle so there is a load transfer that is taking place from rear to front. It interns affects the knuckle as these forces act on the Arm mounting points through the double wishbones.
Considering Maximum acceleration of 1g = 9.81 m/s2
Force at the front side = mass at the rear side of the vehicle × acceleration

Let the mass at the rear side of the vehicle be 0.6 times the total weight
Mass at the rear side of the vehicle=0.6 × 300 =180 kg
Force = 180 × 9.81
Force = 1765.8 N
Now force on 1 wheel =1765.8/2 =882.9 N
Longitudinal Force =882.9 N

B. Wheel Hub
The hub resembles a stepped shaft that gets smaller as it approaches the bearing, or vice versa. Designing a corner with a radius is the most obvious way to reduce stress concentrations at the step, but the hub needs to have a flat face in order to situate the bearing both axially and radially on the hub's spindle. To reduce the stress concentration material was removed directly behind the step to improve the force streamlines.

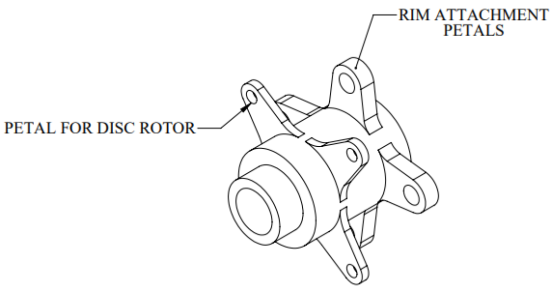

Fig. 7 Wheel Hub

Bump Force = Wheel rate × Travel due to bump = 27× 30 =810 N
Bump Force = 810 N
If the vehicle is banged by another vehicle from the side or if the vehicle has a collision with the fencing from the side, there are chances that the petals might bend. Hence this side impact force must also be considered.
Here the side Impact force is taken to be 2G = 2 × g × vehicle mass
Impact force = 2 × 9.81 × 300 = 5886 N
Impact force on 1 petal = 8829/4 = 1471.5 N
This braking effect must be maintained, and the wheel must deliver an equal and opposing torque. Therefore, while the direction of the torque is opposite, the magnitude is the same.
Torque on wheel petal - = 625 N

C. Manufacturing
Following design and analysis, the steering knuckle's fabrication process is carried out. Using a CNC VMC (Vertical Milling Centre), the upright is constructed. the completed A STEP file of the extracted design was uploaded to the CAM program, where the G and M codes were generated and inputted into the machine. The milling operation was then held over the square block that will become the knuckle and steering arm.

III. FINITE ELEMENTAL ANALYSIS

A. Forces acting on upright –

Based on the loading calculations of upright, the values which are obtained are shown in Table 2

Table 2. Forces acting on upright

Forces	Values
Longitudinal Forces during Braking	882.9 N
Lateral Forces	1175.5 N
Force on the Steering Arm point	1165.52 N
Forces on the caliper mounting points due to torque	1404.49 N

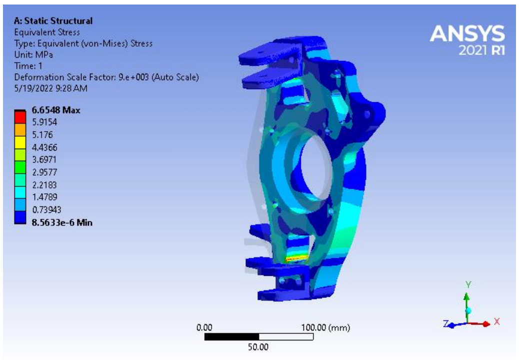

Fig. 8 Von misses stress due to longitudinal force

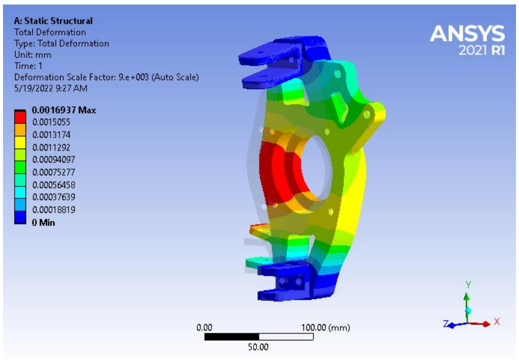

Fig. 9 Max. deformation to longitudinal force

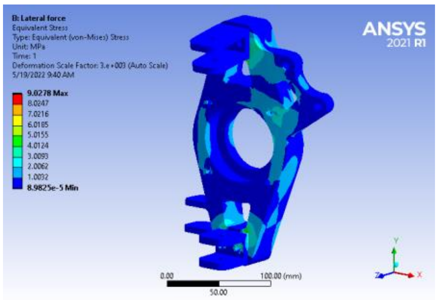

Fig. 10 Stress due to lateral force

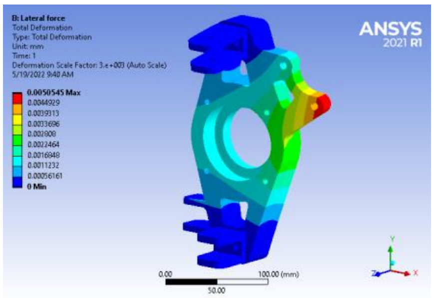

Fig.11 Max. deformation due to lateral force

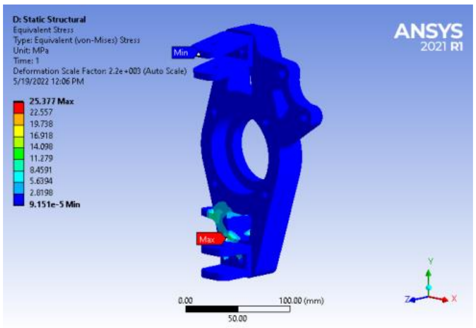

Fig.12 Stress acting on steering arm

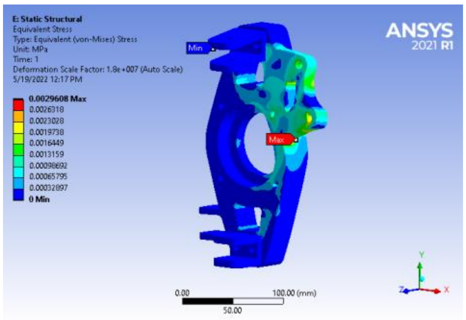

Fig.13 Stress acting caliper mount

Based on the loading calculations of upright, the values which are obtained are shown in table 3

Table 3. Forces acting on upright

Forces	Values
Torque on the Brake Disk Petal	125 N
Torque on the Wheel Petal	125 N
Force due to Side Impact	5886 N

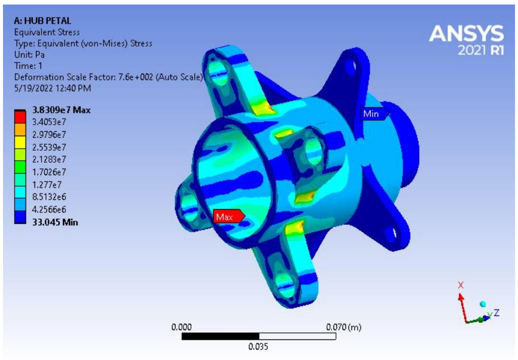

Fig.14 Stress acting on brake petal

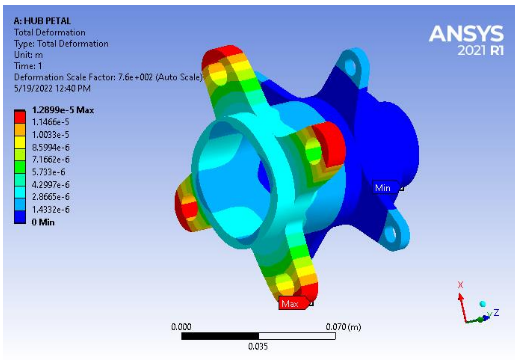

Fig.15 Max. deformation of brake petal

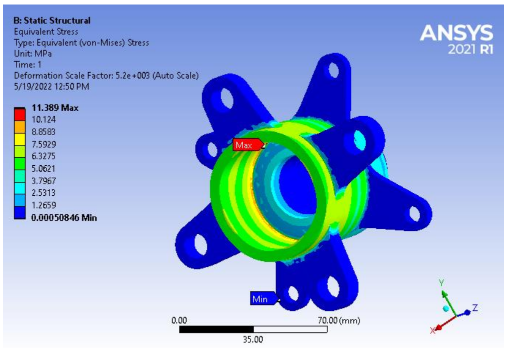

Fig. 16 Stres due to side impact

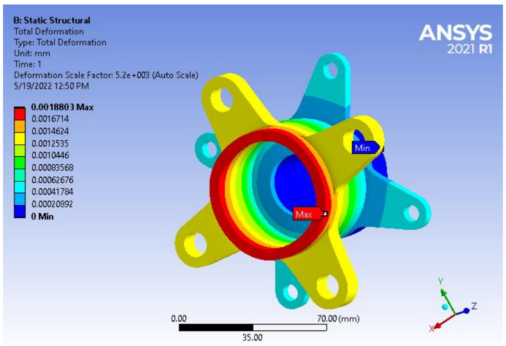

Fig.17 Max. deformation due to side impact

IV. RESULTS

Based on the finite elemental analysis, the following results for different loading conditions are obtained
Results of upright has shown in Table 4

Table 4 Results of upright

Type of force	Results
Longitudinal Forces during Braking	Max Deformation 0.0016 mm Von Misses Stress-6.65 Mpa FOS 12.9
Lateral Forces	Max Deformation -0.005 mm Von Misses Stress-9.02 Mpa FOS 9.3
Force on the Steering Arm point	Max Deformation -0.007 mm Von Misses Stress -25.37 Mpa FOS 3.39
Forces on the caliper mounting points due to torque	Max Deformation -0.0029 mm Von Misses Stress -1.06 Mpa FOS 4.23

The results of the wheel hub have shown in Table 5

Table 5 Results of the wheel hub

Types of force	Results
Torque on the Brake Disk Petal	Max Deformation - 1.28 mm Von Misses Stress - 3.8 Mpa FOS -2.25
Torque on the Wheel Petal	Max Deformation - 4.25 mm Von Misses Stress - 9.83 Mpa

	FOS - 1.96
Force due to Side Impact	Max Deformation -0.0018 mm Von Misses Stress - 13.38 Mpa FOS -7.5

V. CONCLUSION

This paper's goals include designing and producing the upright assembly for the car as well as doing a thorough analysis of the steps that led to the final design. Given that the overall design has been extensively thought out in advance, the manufacturing process is closely monitored, and numerous design aspects have been demonstrated to be effective within the parameters of the vehicle's performance requirements. According to the FEA results, the upright assembly can safely function under real-world track conditions in accordance with performance requirements.

Fig. Final Prototype

REFERENCES:

1. "Design And Analysis Of Steering And Uprights Of Fsae Car." *International Journal of Recent Trends in Engineering and Research*, vol. 3, no. 6, International Journal of Recent Trends in Engineering and Research, June 2017, pp. 290–98. *Crossref*, https://doi.org/10.23883/ijrter.2017.3309.fdatg.
2. Sanjay Yadav, et al. "Design and Analysis of Steering Knuckle Component." International Journal of Engineering Research And, vol. V5, no. 04, ESRSA Publications Pvt. Ltd., Apr. 2016. Crossref, https://doi.org/10.17577/ijertv5is040818.
3. Matushkin, Lev N., et al. "Designing and Manufacturing of the Student Race Car 'Formula Student' Frame (Design and Technological Part)." Innotrans, no. 1, Ural State University of Railway Transport (USURT), 2021, pp. 69–74. Crossref, https://doi.org/10.20291/2311-164x-2021-1-69-74.
4. Ranganathan, Soundararajan, et al. "Design and Analysis of Steering Knuckle at Diverse Strengthening Condition." SAE Technical Paper Series, PA, SAE International, Sept. 2020. Crossref, https://doi.org/10.4271/2020-28-0501.
5. Sanjay Yadav, et al. "Design and Analysis of Steering Knuckle Component." International Journal of Engineering Research And, vol. V5, no. 04, ESRSA Publications Pvt. Ltd., Apr. 2016. Crossref, https://doi.org/10.17577/ijertv5is040818
6. Rajesh kumar, L., et al. "Design, Analysis and Optimization of Steering Knuckle for All Terrain Vehicles." 1st International Conference On Sustainable Manufacturing, Materials And Technologies, AIP Publishing, 2020. Crossref, https://doi.org/10.1063/5.0000044.
7. Bhardwaj, Saksham, et al. "Design and Optimization of Steering Upright to Reduce the Weight Using FEA." SAE Technical Paper Series, PA, SAE International, July 2018. Crossref, https://doi.org/10.4271/2018-28-0081
8. Siva Sankar, S., et al. "Design and Optimization of an All-Terrain Vehicle Upright." International Journal of Vehicle Structures and Systems, vol. 14, no. 6, MAFTREE, Dec. 2022. Crossref, https://doi.org/10.4273/ijvss.14.6.11.